

## SIMS as a Probe of Surface Chemical Kinetics

P. L. RADLOFF and J. M. WHITE\*

Department of Chemistry, University of Texas, Austin, Texas 78712

Received March 14, 1986 (Revised Manuscript Received July 22, 1986)

Elucidating the kinetics of surface chemical reactions on low-area substrates is a difficult problem, particularly when the products remain adsorbed. The difficulty stems in large part from a paucity of techniques that both are sensitive to chemical environment and possess a dynamic range sufficiently large to permit data acquisition on the time scale of reaction. Temperature-programmed desorption (TPD) has provided a majority of the available kinetic data, but is limited to the study of species which desorb from the substrate and can provide information about *surface* kinetics only by inference.

Laser-induced desorption (LID)<sup>1,2</sup> overcomes the shortcomings of conventional desorption methods. In this technique an extremely rapid laser-generated temperature jump induces desorption of all adsorbed species, often in high yield, despite the existence of competing reaction channels.

A variety of other techniques, for example, ultraviolet and X-ray photoelectron spectroscopies (UPS and XPS), extended X-ray absorption fine structure (EXAFS), infrared measurements (IR), and electron energy loss spectroscopy (EELS), provide a direct probe of the surface chemical environment. Due to their generally poor sensitivity, however, it has been possible thus far to implement only a few of these—EELS,<sup>3,4</sup> IR,<sup>5</sup> and angle-resolved photoemission<sup>6</sup>—in a configuration having acceptable time resolution.

Here we focus on another chemically sensitive technique, secondary ion mass spectrometry (SIMS), which has been used in this and other laboratories to monitor surface kinetics.<sup>7-24</sup> SIMS is an extremely sensitive probe, with the ability to detect many surface species at concentrations well below the detection threshold of Auger electron (AES) and other surface spectroscopies. As a consequence of its huge dynamic range, rather short data collection periods (100–200 ms) are required in SIMS experiments. By monitoring secondary ion yields during the course of reaction, information about surface chemical kinetics can be obtained.

The extreme chemical sensitivity of SIMS, while permitting its use as a dynamical probe, also is the greatest complication in its employment. SIMS cross sections are known to vary by as much as 5 orders of

magnitude as the chemical environment and work function are changed.<sup>25</sup> Other difficulties in interpretation arise since SIMS cracking patterns often differ from their gas-phase, electron-impact ionization analogues. The monitoring of cluster ions requires particular care, as clusters may be formed both on and above the surface as a consequence of ion bombardment.<sup>26</sup> In kinetic applications, it is also necessary to verify that the primary ion beam is neither sputtering the surface at a great rate nor inducing chemical reaction. Given the difficulties inherent in the technique, it is clear that SIMS must be used in conjunction with other methods in the characterization of surface kinetics.

This paper describes the utilization of SIMS to help characterize the formation, decomposition, and isotope exchange reactions of alkylidynes, the formation and decomposition of methoxy, and the reaction of hydrogen and oxygen to form water, all on Pt(111). In each case, kinetic parameters are calculated from the time and/or temperature dependence of *calibrated* SIMS

(1) Hall, R. B.; DeSantolo, A. M.; Bares, S. J. *Surf. Sci.* **1985**, *161*, L533.

(2) (a) Cowin, J. P.; Auerbach, D. J.; Becker, C.; Wharton, L. *Surf. Sci.* **1978**, *78*, 545. (b) Wedler, G.; Ruhmann, H. *Surf. Sci.* **1982**, *121*, 464. (c) Burgess, D., Jr.; Hussla, I.; Stair, P. C.; Viswanathan, R.; Weitz, E. J. *Chem. Phys.* **1983**, *79*, 5200. (d) Sherman, M. G.; Kingsley, J. R.; Dahlgren, D. A.; Hemminger, J. C.; McIver, R. T., Jr. *Surf. Sci.* **1985**, *148*, L25. (e) Chuang, T. J.; Seki, H.; Hussla, I. *Surf. Sci.* **1985**, *158*, 525.

(3) Richter, L. J.; Ho, W. J. *Chem. Phys.* **1985**, *83*, 2569.

(4) DuBois, L. H.; Ellis, T. H.; Kevan, S. D. *J. Vac. Sci. Technol. A* **1984**, *3*, 1643.

(5) Burrows, V. A.; Sundaresan, S.; Chabal, Y. J.; Christman, S. B. *Surf. Sci.* **1985**, *160*, 122.

(6) Haight, R.; Bokor, J.; Stark, J.; Storz, R. H.; Freeman, R. R.; Bucksbaum, P. H. *Phys. Rev. Lett.* **1985**, *54*, 1302.

(7) DeLouise, L. A.; Winograd, N. *Surf. Sci.* **1985**, *159*, 199; **1985**, *154*, 79.

(8) Benninghoven, A.; Beckmann, P.; Griefendorf, D.; Schemmer, M. *Appl. Surf. Sci.* **1980**, *6*, 288.

(9) (a) Mohri, M.; Hashiba, M.; Watanabe, K.; Yamashina, T. *Z. Phys. Chem. (Munich)* **1978**, *109*, S233. (b) Mohri, M.; Kakibayashi, H.; Watanabe, K.; Yamashina, T. *Appl. Surf. Sci.* **1978**, *1*, 170.

(10) Fogel, Ya. M. *Int. J. Mass Spectrom. Ion Phys.* **1972**, *9*, 109.

(11) Ogle, K. M.; Creighton, J. R.; Akhter, S.; White, J. M. *Surf. Sci.*, in press.

(12) Creighton, J. R.; White, J. M. *Surf. Sci.* **1983**, *129*, 327.

(13) Creighton, J. R.; Ogle, K. M.; White, J. M. *Surf. Sci.* **1984**, *138*, L137.

(14) Mitchell, G. E.; Akhter, S.; White, J. M. *Surf. Sci.*, in press.

(15) Ogle, K. M.; White, J. M. *Surf. Sci.* **1986**, *165*, 234.

(16) Ogle, K. M.; White, J. M. *Surf. Sci.* **1984**, *139*, 43.

(17) Creighton, J. R.; White, J. M. *Surf. Sci.* **1984**, *136*, 449.

(18) Ogle, K. M.; Creighton, J. R.; Luftman, H. S.; White, J. M. *J. Chem. Phys.* **1983**, *78*, 5839.

(19) Creighton, J. R.; White, J. M. *J. Vac. Sci. Technol. A* **1983**, *1*, 1225.

(20) Creighton, J. R.; White, J. M. *Chem. Phys. Lett.* **1982**, *92*, 435.

(21) Creighton, J. R.; White, J. M. *Surf. Sci.* **1982**, *122*, L648.

(22) Akhter, S.; White, J. M. *Surf. Sci.*, in press.

(23) Belton, D. N.; Sun, Y.-M.; White, J. M. *J. Phys. Chem.* **1984**, *88*, 5172.

(24) Sun, Y.-M.; Belton, D. N.; White, J. M. In *Catalyst Characterization Science*; Deviney, M. L., Gland, J. L., Eds.; ACS Symposium Series 288; American Chemical Society, Washington, DC, 1985; p 80.

(25) Benninghoven, A. *Surf. Sci.* **1975**, *53*, 596.

(26) (a) Winograd, N.; Garrison, B. J.; Harrison, D. E., Jr. *J. Chem. Phys.* **1980**, *73*, 3473. (b) Garrison, B. J.; Winograd, N.; Harrison, D. E., Jr. *J. Chem. Phys.* **1978**, *69*, 1440.

Patricia L. Radloff was born in Cleveland, OH, on April 26, 1955. She received a B.S. from the University of Virginia in 1977 and a Ph.D. in chemistry at the University of Chicago in 1984. Currently she is a Postdoctoral Research Associate with Professor J. M. White at the University of Texas at Austin. Her major research interests center on the chemistry and physics of surfaces and clusters.

John M. White was born November 26, 1938, in Danville, IL. He received a B.S. from Harding College in 1960 and a Ph.D. in chemistry from the University of Illinois in Urbana in 1966. He joined the faculty at the University of Texas at Austin in 1966 and currently holds the Norman Hackerman Professorship in Chemistry. White is a principal editor with the *Journal of Materials Research* and is on the *Journal of Physical Chemistry* advisory board. He has been a visiting staff member at Los Alamos National Laboratory since 1967. His research interests include surface chemistry, the dynamics of surface reactions, and photoassisted catalytic reactions.

signals. Other techniques are used to identify the surface reactants and products. While the SIMS ions detected must be (and are) consistent with these reactions and products, in no case is SIMS used to identify them.

### Experimental Considerations

In this laboratory SIMS is currently being utilized in conjunction with TPD and AES. In other systems being completed, SIMS will be combined with EELS and pulsed laser desorption. These are all ultrahigh vacuum systems capable of reaching  $1 \times 10^{-10}$  Torr.<sup>11-24</sup> Surface cleanliness is monitored with both AES and SIMS. TPD involves a standard e-beam ionizer supplied with the SIMS quadrupole. It is important to recognize the resolution limitations of these quadrupole systems. A particularly noteworthy example for the systems discussed here occurs at  $m/e$  28 where  $\text{CO}^+$ ,  $\text{Si}^+$ , and  $\text{C}_2\text{H}_4^+$  cannot be resolved.

Molecules are adsorbed either by backfilling the chamber (gives more reproducible dosing) or by directing the flux from a capillary array onto the sample (minimizes background). Programmed temperatures between 100 and 1800 K are realized by combining liquid nitrogen cooling with resistive heating.

SIMS is done in a static mode (SSIMS) using Ar ions (600–1000 eV and typically <2 nA). The ion gun, crystal, and mass spectrometer are arranged such that the quadrupole axis is normal to the crystal face and the primary ions are incident at an angle of about  $60^\circ$ . The beam is defocused and rastered across the crystal. The beam effects must be checked for each system studied, but conditions are readily found that give good signal-to-noise and negligible ion-induced surface chemistry and sputtering.

In all experiments in which rate constants are determined, coverages are calibrated using TPD and/or Auger electron spectroscopy. Typically, unknown coverages are established by comparing integrated TPD signals with those corresponding to a known coverage of a particular species, utilizing the stoichiometry of the pertinent surface reaction. Because ion yields are very sensitive to the local surface environment (matrix effects), calibration of SIMS signals must be done carefully and as a detailed function of surface coverage.

### Alkylidynes on Pt(111)

Alkene adlayers on Pt(111) are known to undergo a variety of irreversible transitions as the temperature is increased from 100 to 800 K.<sup>27</sup> Several of these involve the desorption of  $\text{H}_2$  and changes in the SSIMS cracking pattern and ion yield.<sup>12</sup> Of special interest is a relatively stable species observed around 300 K, after loss of a single hydrogen atom. No C–C bond scission occurs and ethylidyne,  $\text{Pt}_3\text{CCH}_3$ , and propylidyne,  $\text{Pt}_3\text{CCH}_2\text{CH}_3$ , are formed from ethylene and propylene, respectively.<sup>27-32</sup> Propylidyne is less stable than

(27) Koestner, R. J.; Van Hove, M. A.; Somorjai, G. A. *J. Phys. Chem.* **1983**, *87*, 203.

(28) Salmeron, M.; Somorjai, G. A. *J. Phys. Chem.* **1982**, *86*, 341.

(29) Koestner, R. J.; Frost, J. C.; Stair, P. C.; Van Hove, M. A.; Somorjai, G. A. *J. Phys. Chem.* **1983**, *87*, 203.

(30) Minot, C.; Van Hove, M. A.; Somorjai, G. A. *Surf. Sci.* **1982**, *127*, 441.

(31) Ibach, H.; Mills, D. L. *Electron Energy Loss Spectroscopy and Surface Vibrations*; Academic: New York, 1982; p 326.

(32) Skinner, P.; Howard, M. W.; Oxtan, I. A.; Kettle, S. F. A.; Powell, D. B.; Sheppard, N. *J. Chem. Soc., Faraday Trans 2* **1981**, *77*, 1203.

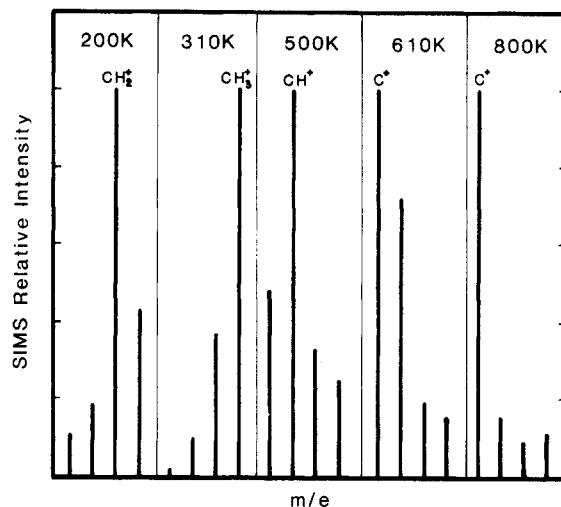


Figure 1. SSIMS fragmentation pattern for ethylene in the  $\text{C}_1$  region ( $m/e$  12, 13, 14, 15) for various temperatures. Ion beam flux was  $3 \text{ nA/cm}^2$ .

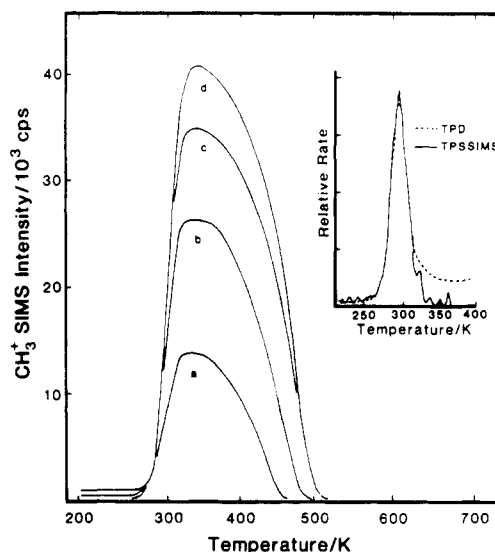


Figure 2. TPSSIMS ( $m/e$  15) of ethylene on Pt(111) as a function of exposure. Exposures in  $L$  are (a) 0.09, (b) 0.17, (c) 0.26, (d) 0.87. The insert compares the derivative with respect to time of curve (d) (solid curve) with the  $\text{H}_2$  TPD peak (dashed line) for saturation coverage. Ion beam flux was  $30 \text{ nA/cm}^2$ .

ethylidyne, and there is some evidence that other reactions compete with propylidyne formation.<sup>33</sup>

Figure 1 shows the SSIMS spectra of an ethylene adlayer at a selection of temperatures. As the system undergoes a change from alkene to alkylidyne the relative intensities of the SSIMS peaks change. In the case of adsorbed ethylene,  $\text{CH}_2^+$  is the major SSIMS fragment, while for ethylidyne  $\text{CH}_3^+$  is the most prominent species. Figure 2 shows the temperature-programmed (TP) SSIMS spectra of  $\text{CH}_3^+$ , which tracks the ethylidyne concentration. The TPSSIMS and TPD data for ethylene and propylene were analyzed to yield activation energies and preexponential factors<sup>11</sup> in a manner similar to that used to characterize TPD data,<sup>34</sup> assuming a first-order dehydrogenation reaction. Kinetic data were also obtained by constructing Arrhenius plots from isothermal SSIMS data. Table I summarizes the ethylidyne and propylidyne formation and decom-

(33) Ogle, K. M.; White, J. M., unpublished results.

(34) Redhead, P. A. *Vacuum* **1962**, *12*, 203.

**Table I**  
Activation Energies and Preexponential Factors for  
Alkylidyne Formation and Decomposition

| parent   | process        | method            | $E_a$ , kcal/mol | $A$ , $s^{-1}$             |
|----------|----------------|-------------------|------------------|----------------------------|
| $C_2H_4$ | F <sup>a</sup> | TPD               | $17 \pm 2$       | $5 \times 10^{12} \pm 1$   |
| $C_3H_6$ | F              | TPD               | $17 \pm 2$       | $5 \times 10^{12} \pm 1b$  |
| $C_2H_4$ | D              | TPD               | $27 \pm 2$       | $6 \times 10^{11} \pm 1$   |
| $C_3H_6$ | D              | TPD               | $23 \pm 2$       | $5 \times 10^{11} \pm 1$   |
| $C_2H_4$ | F              | SIMS              | $15 \pm 2$       | $4 \times 10^{11} \pm 1$   |
| $C_3H_6$ | F              | SIMS              | $18 \pm 2$       | $2 \times 10^{13} \pm 2$   |
| $C_2H_4$ | D              | SIMS              | $17 \pm 2$       | $8 \times 10^8 \pm 2$      |
| $C_3H_6$ | D              | SIMS              | $22 \pm 2$       | $3 \times 10^{11} \pm 2$   |
| $C_2H_4$ | F              | SIMS <sup>c</sup> | $17.3 \pm 2$     | $5.5 \times 10^{11} \pm 1$ |

<sup>a</sup>F = alkylidyne formation; D = alkylidyne decomposition.  
<sup>b</sup>Inferred. <sup>c</sup>Isothermal SSIMS.

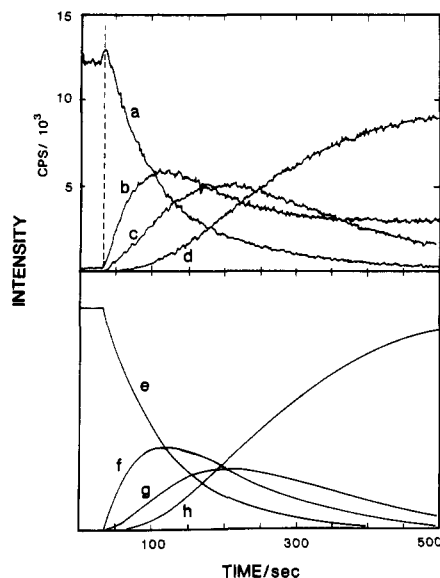


**Figure 3.** Upper panel: a plot of the secondary ion intensities during the isotope exchange reaction at 383K; curves a-d are for  $m/e$  15, 16, 17, and 18, respectively. Incident  $Ar^+$  current density is  $7 \text{ nA/cm}^2$ . The high intensity of  $m/e$  16 at 500 s is due to cracking of  $CD_3$ . Lower panel: calculated results for the model discussed in the text using  $(k\theta_D)^{-1} = 87 \text{ s}$ . Curves e-h represent coverages of  $CH_3$ ,  $CH_2D$ ,  $CHD_2$ , and  $CD_3$ , respectively. Reproduced with permission from ref 13. Copyright 1984, Elsevier, Amsterdam.

position rate parameters. The results of the different methods of analysis are in quite good agreement.

The inset of Figure 2 compares the first derivative of the rising part of the  $CH_3^+$  signal with the first  $H_2$  TPD peak for the highest ethylene exposure, where  $H_2$  desorption is reaction-limited by the ethylene-to-ethylidyne conversion. The two are coincidental, showing that ethylidyne formation kinetics can be reliably followed using the  $CH_3^+$  SIMS signal.

A distinct advantage of SIMS is its combination of mass resolution and high sensitivity. Thus, secondary ion yields may be used to determine the rate of isotope exchange of surface species. H-D exchange in ethylidyne exposed to  $D_2$  at 350 K is shown in Figure 3.<sup>13</sup> The observed decrease in  $CH_3^+$  signal and the increase in the deuterated species may be modeled by the following scheme:

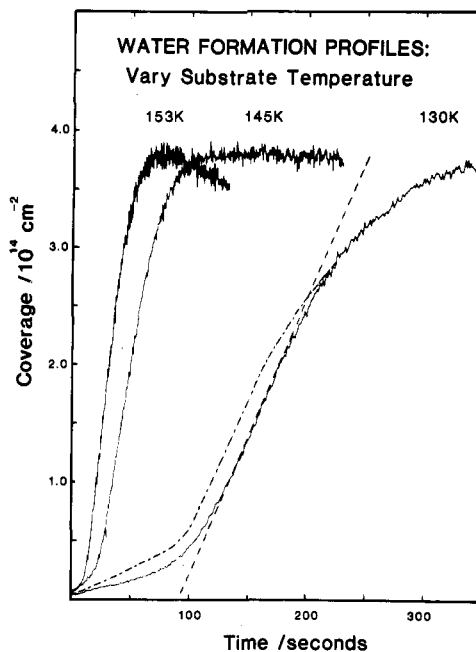
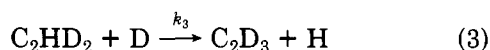
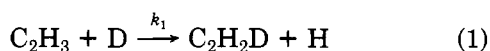


**Figure 4.** Variation of the  $H_3O^+$  SSIMS yield with time as a function of substrate temperature. The initial oxygen coverage was 0.25 monolayer, the  $H_2$  pressure was  $1.1 \times 10^{-7} \text{ Torr}$ , and the  $Ar^+$  beam current was 0.5 nA. The  $H_3O^+$  signal was normalized to that originating from 0.25 monolayer of  $H_2O$ . The slope of the dashed line depicts the maximum rate of water formation at 130 K. The dot-dash curve represents a correction to the 130 K profile arising from variations of the  $H_3O^+$  sensitivity with water coverage. Reproduced with permission from ref 16. Copyright 1984, Elsevier, Amsterdam.

where  $k_1$ ,  $k_2$ , and  $k_3$  each represent the rate constant per hydrogen atom. When one assumes that the concentration of adsorbed deuterium ( $\theta_D$ ) quickly reaches steady state and that  $k_1 = k_2 = k_3 = k$ , the model can be solved explicitly. The best fit to the data, shown in Figure 3, is obtained by using  $(k\theta_D)^{-1} = 87 \text{ s}$ . The excellent agreement between the data and the fit demonstrate that the isotope exchange is well approximated by this simple, statistical model. From temperature-dependent measurements, an activation energy of  $7.2 \pm 0.3 \text{ kcal mol}^{-1}$  has been calculated<sup>15</sup> for this reaction where the products of interest do not desorb.

### Water Formation on Pt(111)

Another interesting example of the power of SIMS involves the interaction of hydrogen, oxygen, and water on Pt(111). The majority of experimental work has focused on reaction above the  $H_2O$  desorption temperature (180 K).<sup>35,36</sup> At lower temperatures<sup>35-41</sup> kinetic data did not exist prior to SIMS measurements in this laboratory.

To study water formation between 130 and 150 K, known oxygen coverages, prepared by standard thermal treatment of adsorbed  $O_2$ ,<sup>42</sup> were reacted with  $H_2$ . The

(35) Norton, P. R. In *The Chemical Physics of Solid Surfaces and Heterogeneous Catalysis*; King, D. A., Woodruff, D. P., Eds.; Elsevier: New York, 1982; Vol. 4, p 27.

(36) Gland, J. L.; Fisher, G. B.; Kollin, E. B. *J. Catal.* **1982**, *77*, 263.

(37) Fisher, G. B.; Gland, J. L.; Schmiegel, S. J. *J. Vac. Sci. Technol.* **1982**, *20*, 518.

(38) Norton, P. R.; Tapping, R. L.; Goodale, J. W. *J. Vac. Sci. Technol.* **1977**, *14*, 446.

(39) Fisher, G. B.; Gland, J. L. *Surf. Sci.* **1980**, *94*, 446.

(40) Fisher, G. B.; Sexton, B. A. *Phys. Rev. Lett.* **1980**, *44*, 683.

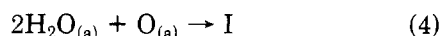
(41) Dawson, P. T.; Peng, Y. K. *Surf. Sci.* **1980**, *92*, 1.

(42) Norton, P. R.; Davies, J. A.; Jackman, T. E. *Surf. Sci.* **1982**, *122*, 103.

reaction was followed by recording the SSIMS signals for  $\text{H}_3\text{O}^+$  and  $\text{H}_2\text{O}^+$  until it was well-established that the protonated water (which is about 14 times as intense) followed the same pattern as the parent ion. The yields of both ions depend slightly on the coverage of oxygen, but reliable rates can nonetheless be extracted.<sup>16</sup>

Water formation profiles as a function of substrate temperature are shown in Figure 4. The reaction profiles are characterized by an induction period, a fast reaction region, and an approach to a saturation value. In the rapid reaction regime the activation energy is  $2.9 \pm 0.3$  kcal/mol. The decay of the signal at 153 K is due to the slow thermal desorption of water.

Earlier studies<sup>21</sup> indicated that an oxygen-covered Pt surface rearranges upon exposure to water to form an intermediate (I), with overall stoichiometry



The induction period observed in the  $2\text{H}_{(a)} + \text{O}_{(a)} \rightarrow \text{H}_2\text{O}_{(a)}$  reaction is attributed to the formation of the same I and the rapid reaction region to the reaction of I with hydrogen to form water.

Isotopic studies of the formation and reaction of the intermediate<sup>14,15</sup> support these ideas. The surface was pre-dosed with  $^{18}\text{O}$ , exposed to  $\text{H}_2^{16}\text{O}$  (to form I), and finally exposed to  $\text{H}_2$ . The induction time decreased and the rate of reaction in the fast reaction region increased as the crystal was exposed to larger amounts of water before the  $\text{H}_2$  dose. These results are consistent with the formation of I in the induction period and its reaction to form water in the rapid reaction regime.

When the SIMS and TPD results are combined, a much clearer picture of the low-temperature water formation reaction has emerged. Rates and activation energies have been measured and a detailed mechanism, including a hydrogen-bonded structure<sup>43</sup> for I, has been proposed<sup>14</sup> that is consistent with all of the available literature.<sup>14,35,39,40</sup> The proposed structure for I involves rows of OH groups with  $\text{H}_2\text{O}$  intercalated between them.

### Methoxy Formation and Decomposition

The decomposition of methanol on many metallic surfaces at low temperatures (usually less than 300 K) leads to a methoxy intermediate.<sup>44-47</sup> In most of the systems which have been studied, the formation and

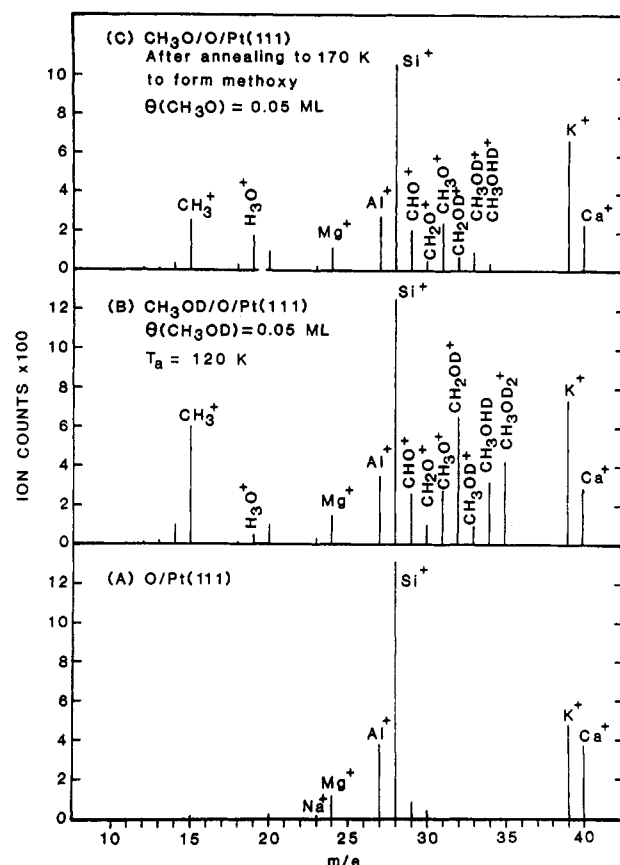


Figure 5. SSIMS ion yields from (a) O/Pt(111), (b) 0.05 monolayer of  $\text{CH}_3\text{OD}$ , and (c) 0.05 monolayer of  $\text{CH}_3\text{O}$  adsorbed on O/Pt(111). Spectra were taken at 120 K and the  $\text{Ar}^+$  beam current was 1.8 nA at 600 eV.

decomposition of the intermediate occurs without reaction-limited product desorption. As a result, investigations have been confined to the use of spectroscopic techniques like HREELS and XPS/UPS, which have assisted in identifying methoxy, but which are incapable of elucidating kinetic parameters. Exceptions include methoxy decomposition on oxygenated Cu(110) and Ag(110), for which reaction-limited product desorption occurs.<sup>44</sup> For these systems, kinetic parameters have been evaluated from TPD data.

Recently, Hall and co-workers have studied the decomposition of methanol on clean Ni(100) by using the laser-induced desorption technique and have obtained kinetic data.<sup>1</sup> Methanol decomposition was self-poisoned and was modeled using coverage-dependent reaction kinetics:

$$k = 2 \times 10^9 \text{ s}^{-1} e^{-(9+4\theta)/RT}$$

where  $\theta$  is the coverage in monolayers and the energy unit is kcal/mol. On the basis of the low value of the preexponential, Hall and co-workers argued in favor of a large entropic barrier to decomposition. Such a barrier could result from the conversion of an initial mobile reactant (methanol) to an immobile (methoxy-like) transition state.

In this laboratory the decomposition of methanol on oxygenated Pt(111) has been examined using isothermal and temperature programmed SSIMS techniques.<sup>22</sup> To determine kinetic parameters for methoxy formation and decomposition, it was necessary to ascertain the coverages of the various species resulting from a specified methanol exposure. This was done by analyzing

(43) (a) Speakman, J. Claire *The Hydrogen Bond*; Monograph for Teachers; The Chemical Society: London, 1975; Vol 27. (b) Olovsson, I.; Jonsson, P. In *The Hydrogen Bond*; Schuster, P., Zundel, G., Sandorfy, C., Eds.; North Holland: New York, 1976; Vol. 2, pp 393-456. (c) Sandorfy, C. *Ibid.*, pp 613-682. (d) Luck, W. A. P. *Ibid.*, pp 527-562.

(44) (a) Wachs, I. E.; Madix, R. J. *Surf. Sci.* 1978, 76, 531; (b) *J. Catal.* 1978, 53, 208.

(45) (a) Bowker, M.; Madix, R. J. *Surf. Sci.* 1980, 95, 190. (b) Goodman, D. W.; Yas, J. T.; Madey, T. E. *Surf. Sci.* 1980, 93, L135. (c) Benziger, J. B.; Madix, R. J. *J. Catal.* 1980, 65, 36. (d) Ko, E. I.; Benziger, J. B.; Madix, R. J. *J. Catal.* 1980, 62, 264. (e) Hansen, D. M.; Stockbauer, R.; Madey, T. E. *J. Chem. Phys.* 1982, 77, 1569. (f) Ko, E. I.; Madix, R. J. *Surf. Sci.* 1981, 112, 373. (g) Miles, S. L.; Bernasek, S. L. *J. Phys. Chem.* 1983, 87, 1626. (h) McBreen, P. H.; Erley, W.; Ibach, H. *Surf. Sci.* 1983, 133, L469. (i) Gates, J. A.; Kesmodel, L. L. *J. Catal.* 1983, 83, 437. (j) Tindall, I. F.; Vickerman, J. C. *Surf. Sci.* 1985, 149, 577. (k) Madix, R. J. In *The Chemical Physics of Solid Surfaces and Heterogeneous Catalysis*; King, D. A., Woodruff, D. P., Eds.; Elsevier: New York, 1982; Vol 4.

(46) Sexton, B. A. *Surf. Sci.* 1981, 102, 271.

(47) (a) Sexton, B. A.; Rendulic, K. D.; Hughes, A. E. *Surface Sci.* 1982, 121, 181. (b) Rendulic, K. D.; Sexton, B. A. *J. Catal.* 1982, 78. (c) Solymosi, F.; Berko, A.; Tarnocz, T. I. *Surf. Sci.* 1984, 141, 533.

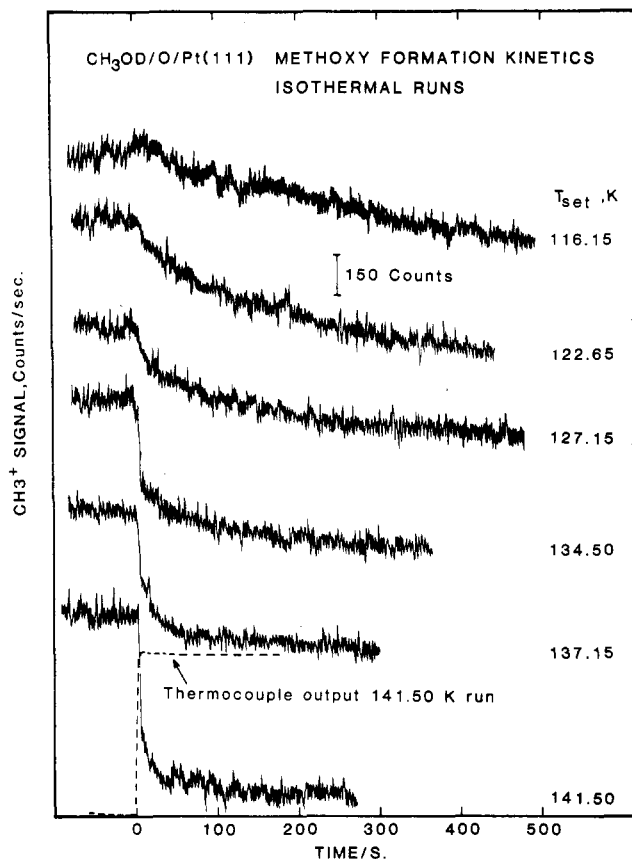
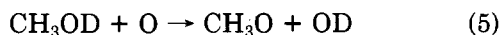


**Figure 6.** Decay of the CH<sub>3</sub><sup>+</sup> ion intensity during isothermal methoxy formation at different temperatures on O/Pt(111). The initial CH<sub>3</sub>O<sub>(a)</sub> coverage was 0.05 monolayer for all runs. The Ar<sup>+</sup> beam current was 1 nA at 600 eV. The dashed line represents the thermocouple output for the 141.5 K experiment. The almost constant signal at 200 s for this experiment is about half the total initial signal.

TPD data constrained by the stoichiometry of the methanol decomposition reaction.<sup>22</sup>

The reaction between surface methanol and surface oxygen was studied by preparing oxygenated surfaces, as in the water formation experiments, and dosing with CH<sub>3</sub>OH. A SSIMS spectrum for the oxygen-covered Pt(111) surface is shown in Figure 5. While an AES spectrum of the same surface gave no indication of impurities, Si<sup>+</sup> and a number of trace metal ions were detected by SSIMS. Exposure to methanol gave rise to several new peaks (center frame of Figure 5). Annealing to 170 K to produce methoxy generated no new features, but the intensity of most of the alcohol derived peaks decreased.

The formation and decomposition of methoxy is reflected in variations of the CH<sub>3</sub><sup>+</sup> SSIMS signal. Isotopically labeled methanol decomposition,



at 125 K is heralded by a rise in D<sub>3</sub>O<sup>+</sup> signal from OD and a drop in methyl ion yield.

Kinetic parameters for methoxy formation were determined from the isothermal SSIMS data (Figure 6). The Arrhenius activation energy is  $5.5 \pm 0.7$  kcal/mol. The preexponential, determined by assuming a second-order rate expression of the type  $R = k \times (\text{CH}_3\text{OD})(\text{O})$ , was  $1.5 \times 10^{-7 \pm 0.6}$  cm<sup>2</sup> s<sup>-1</sup> mol<sup>-1</sup>. If the reaction is presumed to be first order, the preexponential becomes  $1 \times 10^7$  s<sup>-1</sup>. The methoxy formation

parameters are similar to those determined for methanol decomposition on Cu(100).<sup>44b</sup> The data obtained in this work are consistent with the interpretation espoused by Hall.<sup>1</sup> The value of the preexponential for methoxy formation on O/Pt(111) is low compared with that expected for an ideal second-order reaction ( $10^{-3}$ ) and an attempt to fit the entire reaction curve, Figure 6, using the simple Arrhenius model was unsuccessful. A similar analysis, assuming first-order kinetics, was performed for methoxy decomposition, yielding an activation energy of  $11.4 \pm 0.5$  kcal/mol and a preexponential  $5.3 \times 10^{10 \pm 1}$  s<sup>-1</sup>.

### Concluding Remarks

As is demonstrated by the examples given above, SIMS measurements afford insights not attainable with other techniques. The combination of temperature-programmed desorption with isothermal and temperature-programmed SIMS has yielded the fullest kinetic description of both the water formation reaction and the alkylidyne formation and decomposition reactions. SSIMS measurements have provided the only kinetic data for isotope exchange in alkylidynes on single crystals, and have complemented existing studies of methanol decomposition. In another interesting example not discussed here, temperature-programmed SIMS analysis of thin-film models of Pt/TiO<sub>2</sub> catalysts<sup>23,24</sup> provide the strongest available evidence for encapsulation as a major component of the strong metal-support interaction.<sup>48</sup>

Advantages of the technique include the ease with which a SIMS apparatus may be incorporated in a standard UHV chamber and its high sensitivity for a variety of surface species, of which Ti<sup>+</sup> is a good example. On the other hand, SIMS is ill-suited for monitoring many species, for example, carbon monoxide, due to an extremely low cross section for ion production. While the signal to noise ratio of a low-yield ion may be improved by increasing the primary ion current, it is necessary to demonstrate that neither ion-induced chemistry nor excessive sputtering occurs as a result. A significant complication of the SIMS technique is the variation of the secondary ion creation cross section with surface composition. As a consequence, coverages determined using SIMS must be carefully calibrated as a detailed function of coverage of all species present.

SIMS probes of kinetics are by no means limited to the observation of positive ions, although at this time, the understanding of negative ion formation and cracking patterns is very incomplete. Negative SIMS is, however, a very sensitive means of detecting surface carbon, and may be useful in the study of systems in which carbon is either a contaminant or a reaction product. The observation of clusters in secondary ion spectra suggests that SIMS may be a useful probe of weakly associated complexes. Interpretation of such data, however, requires that complexes originating on the surface be distinguished from those which are formed by ion-molecule reactions in the vapor.

(48) (a) *Metal-Support and Metal Additive Effects in Catalysts*; Imelik, B. et al., Eds.; Elsevier: Amsterdam, 1982. (b) Huizinga, T. Dissertation, Eindhoven University of Technology, 1983. (c) Jiang, X.-Z.; Hayden, T. F.; Dumesic, J. A. *J. Catal.* 1983, 83, 68. (d) Reasco, D. E.; Haller, G. L. *J. Catal.* 1983, 82, 279. (e) Vannice, M. A.; Twu, C. C. *J. Catal.* 1983, 82, 213. (f) Short, D. R.; Mansour, A. N.; Cook, J. W., Jr.; Sayers, D. E.; Katzer, J. R. *J. Catal.* 1983, 82, 299. (g) Fang, S.-M.; White, J. M. *J. Catal.* 1983, 83, 1. (h) Tanaka, K.; White, J. M. *J. Catal.* 1983, 79, 81. (i) Baker, R. T. K. *J. Catal.* 1980, 63, 523. (j) Fung, S. C. *J. Catal.* 1982, 76, 225.

The work described herein raises a number of questions. Why is  $\text{CH}_3^+$  the most intense fragment in the ethylidyne spectrum and  $\text{CCH}_3^+$  the greatest in that of propylidyne? Why does the  $\text{CH}_3\text{O}^+$  signal decrease as methanol is converted to methoxy? Why is the  $\text{H}_3\text{O}^+$  signal derived from water much stronger than that of hydroxyl? These and other observations challenge our understanding of the process of secondary ion creation.

Prospects for future research using SSIMS and related techniques are excellent. Investigations of the decomposition of alkenes on Ru(001) and of ketene ( $\text{CH}_2\text{CO}$ ) on Ru(001) and Pt(111) are in progress in this laboratory. These studies represent an attempt to gain insight into the mechanism of the Fischer-Tropsch synthesis through consideration of the decomposition and reaction of small hydrocarbons and hydrocarbon fragments on single-crystal surfaces. Additional work in progress combines the SSIMS, EELS, and TPD techniques in the study of the reactions of  $\text{H}_2\text{S}$  on oxygenated Pt(111). Preliminary results indicate that water is formed at 100 K with high yield. Future in-

vestigations of strong metal-support interactions include model catalyst studies using  $\text{TiO}_2$  in which an alkali metal is deposited prior to growth of the Pt or Rh overlayer.

Secondary neutral mass spectrometry, a technique closely related to SIMS, holds great promise as a tool in the investigation of surface reaction kinetics. In this method, sputtered neutrals, which comprise a large fraction of the particles ejected in SIMS, are ionized and mass analyzed. Although observed yields depend on the choice of ionization source (electron impact or photoionization), both types of ionization, as well as the sputtering process, are fairly well-understood. As a result, it should be possible to relate ion yields to the density of surface species and hence to more accurately quantify reaction rate measurements.

*We gratefully acknowledge the contributions of our colleagues, who have pioneered the use of secondary-ion mass spectrometry in the study of surface kinetics. This research was supported by the National Science Foundation (NSF CHE8505413), the Office of Naval Research, and the Robert A. Welch Foundation.*